ECCOMAS

Proceedia

A TWO-STEP APPROACH FOR THE SEISMIC ASSESSMENT OF MASONRY STRUCTURES ACCOUNTING FOR THE ACTUAL MASONRY PATTERN

Simon Szabó[1], Marco F. Funari[2], Antonio Maria D'Altri[3], Stefano de Miranda[3], and Paulo B. Lourenço[1]

[1] ISISE, Department of Civil Engineering, University of Minho Campus de Azurém, 4800-058 Guimarães, Portugal
e-mail: simon.szabo117@gmail.com, pbl@civil.uminho.pt

[2] School of Sustainability, Civil and Environmental Engineering, University of Surrey, Guildford GU2 7XH, UK
e-mail: m.funari@surrey.ac.uk

[3] Department of Civil, Chemical, Environmental, and Materials Engineering, University of Bologna, Italy
e-mail: am.daltri@unibo.it, stefano.demiranda@unibo.it

Abstract

Seismic assessment of masonry structures is a pressing concern in the scientific community. Over the last few decades, significant progress has been made in developing numerical modelling strategies for masonry. However, due to the unique mechanics of masonry, which exhibit a quasi-brittle and anisotropic behaviour, there is no trade-off between accuracy and computational efficiency when conducting numerical simulations of masonry structures. This study proposes a new approach to conduct in-plane numerical simulations of masonry structures, which couple limit and pushover analyses considering the actual masonry pattern. The first step of the procedure involves a block-based limit analysis, which considers the actual masonry pattern. Macroblocks, i.e., the portions which compose the collapse mechanism, are then identified using an ad-hoc algorithm that searches for the pivot point of the obtained failure mechanisms. In the second step, a pushover analysis is conducted on the simplified structure composed of macroblocks, considered as continuum bodies, interacting via frictional interfaces. The proposed approach is preliminary tested on two structural-scale benchmarks made of dry-stack masonry, showing promising results.

Keywords: Masonry Pattern, Historic Masonry, Rapid Seismic Assessment.

1   INTRODUCTION

Over the past few decades, significant progress has been made in reliably assessing the structural integrity of historic masonry buildings. To accurately predict damage scenarios and ensure structural integrity safety, it is important to use high-fidelity geometrical re-constructions along with appropriate numerical approaches [1–5]. Over the past few decades, there has been extensive use of numerical models for the nonlinear analysis of historical masonry structures. These models are typically based on either micro (block-based) or continuous approaches [4,6–11]. Block-based methods are particularly suitable for modelling large displacement static or dynamics problems. However, continuous representation of masonry at the material scale is still the most used strategy because of the large spread among practitioners and researchers.

Compared to advanced numerical methods, which are typically implemented within computational schemes either based on the Discrete Element Method (DEM) or Finite Element Method (FEM), other analytical approaches allow for rapid and computationally efficient seismic assessment of masonry buildings [12–14]. In particular, structural engineers often use analytical approaches based on limit analysis (LA) theorems that have the great advantage of being independent of many material properties but inevitably rely on a very simplified material model [15–17].

Analytical and numerical approaches have their own strengths and weaknesses, i.e. micro- or continuum approaches require a significant amount of input data for the nonlinear characterization of masonry, making the structural assessment of historical masonry structures economically expensive and time-consuming. In contrast, analytical approaches are based on certain assumptions and can be widely used to study local failure mechanisms, but they are not sufficient for a global assessment. Thus, a combination of different approaches may be necessary to comprehensively understand the behaviour of historical masonry structures under horizontal loading. To this end, new computational modelling strategies are investigating hybrid approaches combining analytical/analytical [12], analytical/numerical [10], or numerical/numerical approaches [18].

The first attempt to define a workflow based on a two-stepped analysis has been proposed in [18]. To analyze the behaviour of the structure, a 3D finite element (FE) model is first used to perform linear-elastic analysis. Following this, a pushover analysis of the single macro-elements is conducted. The pushover analysis results are then compared to the collapse loads obtained through limit analysis. These comparisons have shown that the nonlinear finite element model is capable of providing accurate simulations of the actual response of masonry elements. Other authors [19] proposed modelling approaches analyzing structures with nonlinear static or dynamic analysis to detect the most likely collapse mechanisms. The upper bound limit analysis method was applied in the second step to compute the maximum horizontal acceleration that the structure can withstand analytically. In [10], the authors proposed a two-stepped analysis in which a nonlinear static analysis was performed to identify the failure mechanism's geometry. Then, the second step aimed to refine the geometry of the failure mechanism through an optimization based on limit analysis and genetic algorithm, which explores the research panorama of kinematically compatible solutions. In [19], the authors recently proposed a new workflow based on the adaptive limit and pushover analyses. First, limit analysis was used to identify the position of the cracked surfaces by adopting an adaptive NURBS approach. Subsequently, the geometry of the collapse mechanism was imported into FE software to perform a nonlinear static analysis simulation by adopting a hardening plasticity model and cohesive-frictional contact based on the interfaces between macroblocks.

The review of existing literature highlights the absence of two-step procedures that take into account the actual masonry pattern. To address this gap, the present study aims to develop a

comprehensive workflow that includes micro-LA, macroblock identification of the failure mechanism, and nonlinear pushover analysis. This approach is designed to enable the rapid seismic assessment of masonry walls that are characterized by irregular masonry patterns [20,21]. This paper is organized as follows: Section 2 briefly describes the methodology implemented. Section 3 presents some preliminary results obtained by adopting the proposed procedure, and finally, the conclusions are discussed in Section 4.

2 METHODOLOGY

This section outlines the theoretical foundation of the proposed two-step approach. The first step involves solving the structural benchmark using a micro-LA formulation, where the displacement field outcomes are used to identify groups of blocks that behave as macroblocks. Finally, a pushover analysis is conducted on the simplified structure composed of macroblocks, considered as continuum bodies, interacting via frictional interfaces. Accordingly, the load-displacement curve of the structure, typically used to assess the structural performance, is obtained.

2.1 Micro-LA Formulation

In the micro-LA formulation, dry-stack assemblage is represented by rigid blocks connected by frictional contact interfaces with a non-associative flow rule, with zero dilation (Figure 1a).
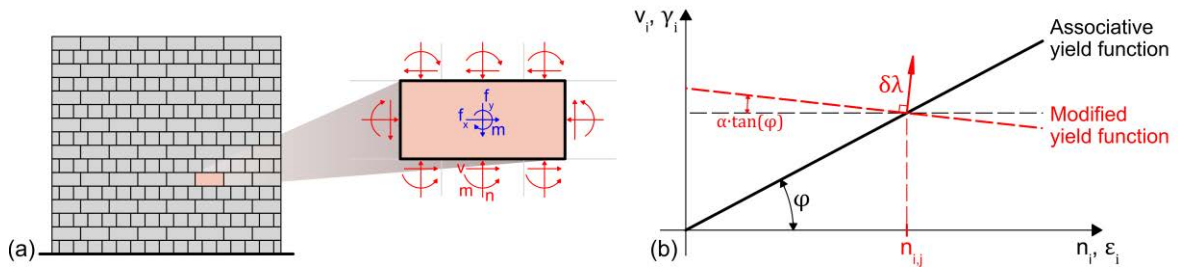

Figure 1:(a) Dry-stack masonry wall; (b) Modification of yield function for the non-associative solution

The solution scheme proposed in [21], involving a non-associative frictional flow rule consisting of sequential solutions of linear programs, is adopted (Figure 1b). At each iteration, a linear program is defined as follows:

Maximize $\quad \lambda$

Subject to $\quad \mathbf{Bq} - \lambda \mathbf{f}_L = \mathbf{f}_D$ $\qquad(1)$

$\qquad\qquad \mathbf{C}^T [\mathbf{q} - \mathbf{c}] \leq 0$

where λ is the load multiplier and $\mathbf{q}$ the vector of unknown contact forces, $\mathbf{f}_L$ and $\mathbf{f}_D$ are the live and dead loads, $\mathbf{c}$ is the cohesion vector, $\mathbf{B}$ and $\mathbf{C}$ are the equilibrium and yield constraints matrices. The first constraint represents the equilibrium of forces, whereas the second is the condition for yielding (failure) of the interfaces.

The yield conditions are updated at each iteration based on the normal forces at the previous iterations:

$$v_{i,j} \leq c_i + \alpha \cdot \mu_i \cdot n_{i,j}$$
$$c_{i,j+1} = c_i^0 + (1+\alpha) \cdot \left(\beta \cdot n_{i,j} + (1-\beta) \cdot n_{i,j-1} \right) \cdot \tan(\varphi_i) \qquad(2)$$

here φ is the frictional angle, $v_{i,j}$ and $n_{i,j}$ are the shear and normal forces of the *i-th* interface at the *j-th* iteration. α and β are algorithm parameters set to 0.01 and 0.6, respectively.

Finally, the steps of the iterative algorithm are the following [21]:

1. Set up the limit analysis problem, according to Eq. (1) with associative-frictional yield conditions.
2. Solve the LP and save the load multiplier λ_0 and the normal forces at each interface $\boldsymbol{n_0}$.
3. Modify the shear failure condition based on the previous iteration, according to Eq. (2).
4. Solve the LP with the modified yield conditions in Step 3) and save the load multiplier λ_j and normal contact forces $\boldsymbol{n_j}$.
5. If the exit condition $\left(\dfrac{\left| \lambda_j - \lambda_{j-1} \right|}{\lambda_j} \leq \text{tolerance} \right)$ is true, the algorithm terminates. Else, repeat from Step 3).
6. Calculate the kinematic variables (displacement rates) from the dual linear program.
7. Calculate the kinematic variables (displacement rates) from the dual linear program.

The algorithm has been implemented in a custom computer code in the JAVA programming language and the interior point LP solver of the MOSEK optimization software (https://www.mosek.com/) has been used for the subsequent numerical studies.

2.2 Macroblock identification

In order to automatically create a macroblocks configuration from the outcomes of the micro-LA solution, two criteria have been introduced (Figure 2). The algorithm aims to detect blocks which behave as a macroblock.
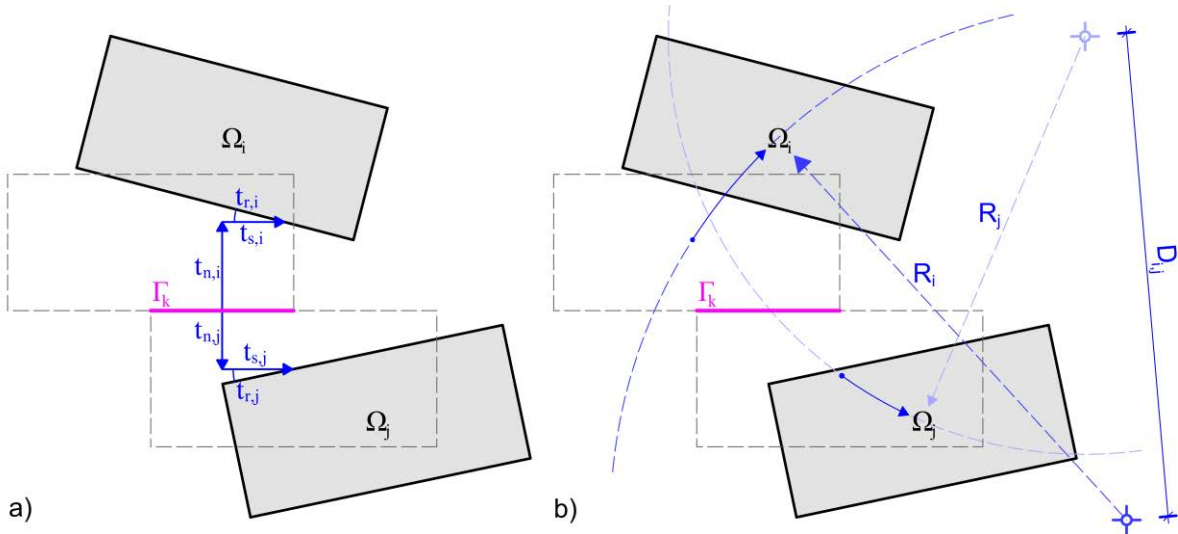

Figure 2. Macroblock definition criteria by a) relative interface displacement, b) centre of rotation

The relative interface displacement criterion (Figure 2a) limits one interface's relative displacement in the normal and transversal directions and the relative rotation with the tolerance values $t = \left\{ tol_n, tol_s, tol_r \right\}$:

$$\left| t_{n,i} - t_{n,j} \right| \leq tol_n$$

$$\left| t_{s,i} - t_{s,j} \right| \leq tol_s \qquad\qquad (3)$$

$$\left| t_{r,i} - t_{r,j} \right| \leq tol_r$$

where $t_{n,i}$ denotes the normal displacement of the *i-th* block from the *k-th* interface. It should be noted that the tolerance values are normalized by the maximum displacement of the structure.

The centre of rotation criterion (Figure 2b) limits the maximum distance of the centre of rotation of two adjacent blocks with a tolerance value tol_D:

$$D_{i,j} \leq tol_D \tag{4}$$

where $D_{i,j}$ represents the distance between the centres of rotation of block i and j. This condition provides that in the areas characterized by distributed sliding unrealistic interlocking of macroblocks is not created. When all the inequalities of Eq. (3) and Eq. (4) hold true, two adjacent blocks are merged in one macroblock. Looping through all the interfaces of the structure and applying the above-described conditions, the macroblock representation of the whole structure can be created. The above definition provides that a set of blocks moving like rigid bodies are segmented in the same macroblock, while regions characterized by distributed sliding are represented by small segments, or even individual blocks. In this study, only tol_n and tol_D have been considered as a variable, while the other two tolerance values have been set to a very high number.

2.3 FE pushover analysis

In this study, pushover analyses are conducted on structures composed of macroblocks within a FE framework. Particularly, macroblocks are considered as linear elastic continuum bodies, discretized via solid FEs (4-node tetrahedrons), which interact through zero-thickness frictional interfaces. In this context, a node-to-surface contact-based frictional formulation is assumed for the macroblock interfaces. The contact constraint is enforced via the Lagrange multiplier method, while a penalty friction formulation, only defined by the friction coefficient and a slip tolerance, is adopted to model the slipping between macroblocks.

Each pushover analysis is composed of two steps. Firstly, gravity loads are applied to each macroblock. Secondly, mass-proportional horizontal loads are applied to each macroblock employing a quasi-static dynamic implicit algorithm. This approach allows extraction of the structure's pushover curve, which is typically used to perform structural assessments and seismic verifications.

3   RESULTS

The results of two structural-scale benchmarks made of dry-stack masonry are herein presented and discussed. The first benchmark consists of a shear wall with four evenly distributed openings (Figure 3a), taken from Ferris et al. [23], and besides others, also adopted by [22,24]. The wall thickness is 100 mm and is constituted by a regular masonry pattern with block dimensions $400 \times 175 \times 100$ mm^3. In accordance with [23], a friction coefficient of 0.65 and specific weight of 25 kN/m^3 is considered in the analyses.

The second benchmark, represented in Figure 3b, is a slender shear wall with one opening placed in the middle. The wall's thickness is 300 mm and is constituted by an irregular, coursed-rectangular masonry pattern with block widths and heights ranging between 120-260 mm and 90-130 mm, respectively. A friction coefficient of 0.75 and a specific weight of 19.4 kN/m^3 is considered.

For both benchmarks, Young's modulus equal to 3.5 GPa and Poisson's ratio equal to 0.2 have been assumed for both locks and macroblocks. As follow, the results of micro-LA and micro-FE (where each block is modelled individually) are shown and compared with several macroblocks arrangements (obtained with different tolerance settings) in terms of pushover curves and collapse mechanisms(Figure 4). As can be noted in Figure 4, most of the macroblocks configurations show a maximum base shear substantially included between the range identified by the micro-LA (upper bound) and the micro-FE (lower bound), except for the cases

with no condition on tol_n (as well as the ones with $tol_n = 22.5 \cdot 10^{-6}$ and $tol_D = 900$ mm or no condition on tol_D) in the first benchmark (Figure 4a), which correspond to a discretization of only one macroblock (not realistic). Indeed, only one macroblock leads to a trivial collapse mechanism characterized by the horizontal slipping of the macroblock, considerably far from the expected collapse mechanisms (Figure 5, Figure 6 and Table 1).
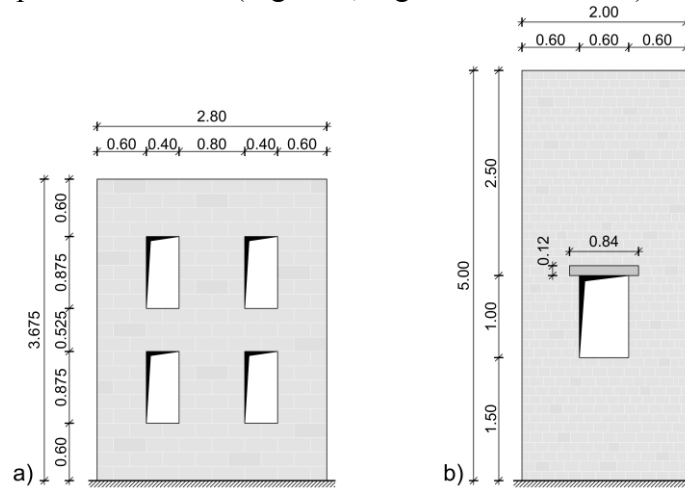

Figure 3. Geometric representations of the analyzed masonry specimens, a) regular masonry [22], b) irregular masonry.

a)

b)
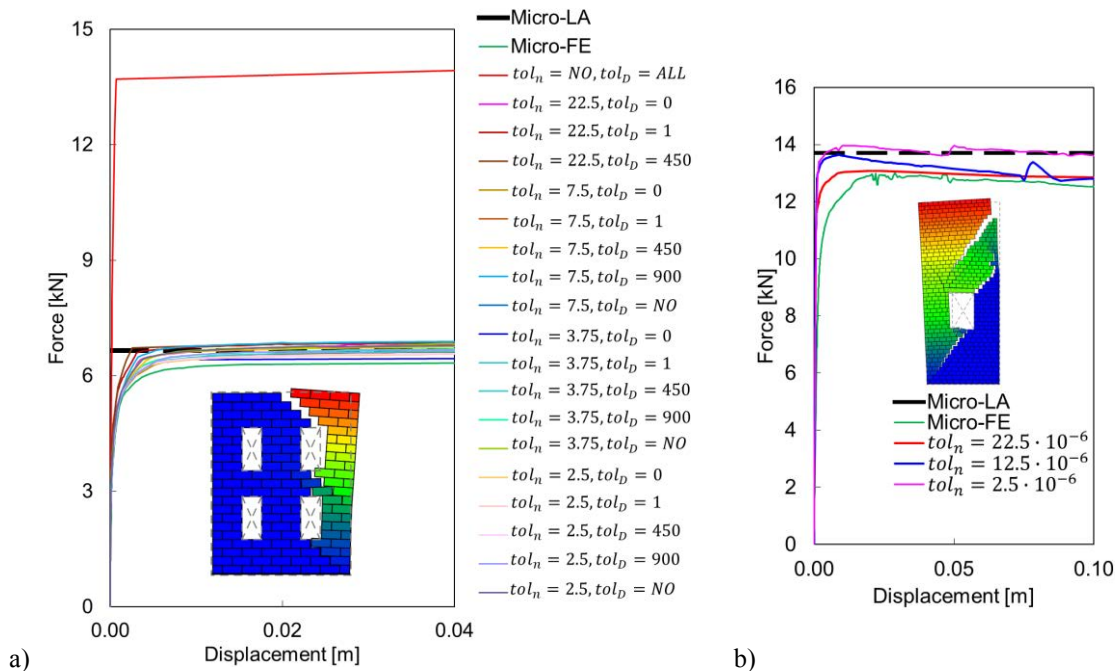
Figure 4. Pushover curves for a) the first benchmark, and for b) the second benchmark. In subfigure a), tolerance values are shown in a concise manner. Refer to Table 1 for further details.

As can be noted in Figure 4, the maximum base shear obtained in the pushover analyses with macroblocks are substantially included between the micro-LA (upper bound) and the micro-FE (lower bound), except for the cases with no condition on tol_n (as well as the ones with $tol_n = 22.5 \times 10^{-6}$ and $tol_d = 600$ mm or no condition on tol_D) in the first benchmark (Figure 4a) which are basically composed of a unique macroblock. In fact, only onw macroblock leads to a trivial collapse mechanism characterized by the horizontal slipping of the macroblock, considerably far from the expected collapse mechanisms.

In particular, it should be pointed out that the difference in shear peak load between micro-LA and micro-FE is substantially small for both benchmarks (Figure 4), and so all the non-trivial macroblock solutions appear close to the expected shear capacity. This is also confirmed by the collapse mechanisms, which are very similar for micro-LA, micro-FE and non-trivial macroblock configurations (Figure 5, Figure 6 and Table 1).
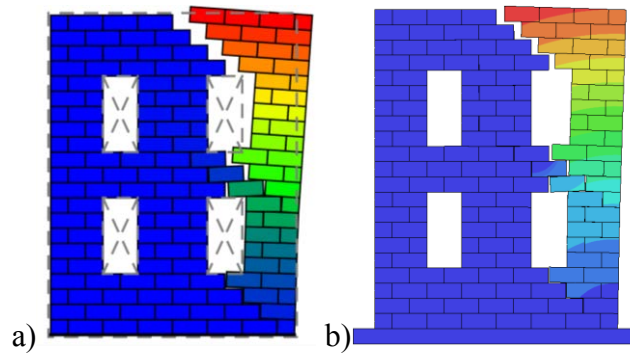

a)   b)

Figure 5. Collapse mechanisms of the first benchmark for a) micro-LA, and b) micro-FE models.

Table 1. Collapse mechanisms of macroblock arrangements of the first benchmark for different tolerance values.

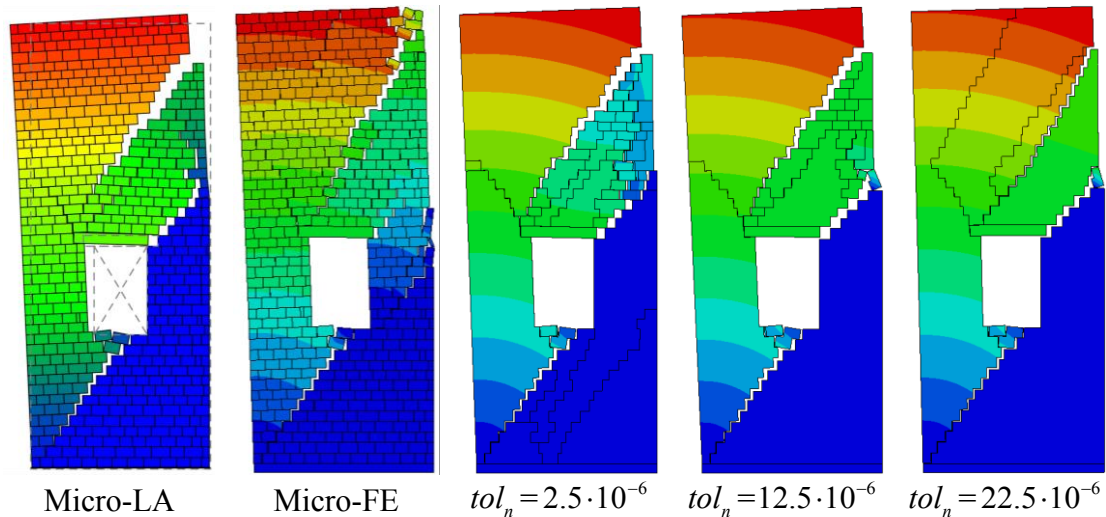|		Centre of rotation criterion (tol_D)				
		$0\ mm$	$1\ mm$	$450\ mm$	$900\ mm$	No condition
Relative interface displacement criterion (tol_n)	$2.5 \cdot 10^{-6}$					
	$3.75 \cdot 10^{-6}$					
	$7.5 \cdot 10^{-6}$					
	$22.5 \cdot 10^{-6}$					
	No condition					

| Micro-LA | Micro-FE | $tol_n = 2.5 \cdot 10^{-6}$ | $tol_n = 12.5 \cdot 10^{-6}$ | $tol_n = 22.5 \cdot 10^{-6}$ |

Figure 6. Collapse mechanisms of the second benchmark. Macroblocks are defined through different tol_n tolerance values ($tol_D = 450$ mm).

Finally, two considerations on the pushover curves should be pointed out.
- First, small jumps can be observed in the pushover curves of the second benchmarks (Figure 4b). This is due to the interlocking between blocks and small macroblocks that rotate.
- Second, differences in the pre-peak response between micro-FE and macroblock solutions can be observed. In particular, the pre-peak behaviour of macroblock solutions is typically stiffer than micro-FE. However, it should be highlighted that the penalty factors used in the contact-based friction formulation do not significantly impact the overall stiffness. This difference is then mainly ascribable to the fact that zero-thickness interfaces are here assumed as no-tension. Consequently, more no-tension interfaces (as in micro-FE) make the structure more deformable. This fact can be overcome by considering cohesive-frictional joints, as in more common masonries with mortar joints.

4   CONCLUSION

This paper outlines a two-step method for performing numerical simulations of in-plane masonry structures. The method incorporates micro-LA and FE pushover analyses accounting for the masonry pattern. In the first step, micro-LA is conducted, accounting for the real pattern. An algorithm is used to identify macroblocks, i.e. the components that make up the collapse mechanism. A parametric study investigates the tolerance value's influence on identifying macroblocks. Overall, more accurate macroblocks definitions do not affect the response in terms of peak load. In contrast, it influences the initial stiffness of the loading-displacement curves. The computational cost of the simulations is strongly decreased when the proposed formulation is adopted as an alternative to the pushover on assuming the Micro-FE model. Future developments will include (i) an assessment of the reliability of the proposed method for other structural benchmarks, (ii) a generalization of the proposed method even for out-of-plane loading conditions, which typically show the most destructive effects on historical masonry structures, (iii) quantification of the computational efficiency of the proposed formulation with respect to the Micro-FE model.

ACKNOWLEDGEMENTS

REFERENCES

[1] M. Shaqfa, K. Beyer, A virtual microstructure generator for 3D stone masonry walls, Eur. J. Mech. - A/Solids. 96 (2022) 104656. https://doi.org/https://doi.org/10.1016/j.euromechsol.2022.104656.

[2] S. Zhang, M. Hofmann, K. Beyer, A 2D typology generator for historical masonry elements, Constr. Build. Mater. 184 (2018) 440–453. https://doi.org/10.1016/J.CONBUILDMAT.2018.06.085.

[3] B. Pantò, F. Cannizzaro, S. Caddemi, I.C.-A. in Engineering, undefined 2016, 3D macro-element modelling approach for seismic assessment of historical masonry churches, Elsevier. (n.d.).

[4] B. Pulatsu, S. Gonen, F. Parisi, E. Erdogmus, K. Tuncay, M.F. Funari, P.B. Lourenço, Probabilistic approach to assess URM walls with openings using discrete rigid block analysis (D-RBA), J. Build. Eng. 61 (2022) 105269. https://doi.org/https://doi.org/10.1016/j.jobe.2022.105269.

[5] M.F. Funari, B. Pulatsu, S. Szabó, P.B. Lourenço, A Solution for the Frictional Resistance in Macro-Block Limit Analysis of Non-periodic Masonry, STRUCTURES. (2022).

[6] A.M. D'altri, V. Sarhosis, G. Milani, J. Rots, S. Cattari, S. Lagomarsino, E. Sacco, A. Tralli, G. Castellazzi, S. De Miranda, Modeling Strategies for the Computational Analysis of Unreinforced Masonry Structures: Review and Classification, 27 (2020) 1153–1185. https://doi.org/10.1007/s11831-019-09351-x.

[7] V. Sarhosis, J. V Lemos, K. Bagi, Chapter 13 - Discrete element modeling, in: B. Ghiassi, G.B.T.-N.M. of M. and H.S. Milani (Eds.), Woodhead Publ. Ser. Civ. Struct. Eng., Woodhead Publishing, 2019: pp. 469–501. https://doi.org/https://doi.org/10.1016/B978-0-08-102439-3.00013-0.

[8] M.F. Funari, S. Spadea, P. Lonetti, F. Fabbrocino, R. Luciano, Visual programming for structural assessment of out-of-plane mechanisms in historic masonry structures, J. Build. Eng. 31 (2020). https://doi.org/10.1016/j.jobe.2020.101425.

[9] N. Hoveidae, A. Fathi, S. Karimzadeh, Seismic damage assessment of a historic masonry building under simulated scenario earthquakes: A case study for Arge-Tabriz, Soil Dyn.

Earthq. Eng. 147 (2021) 106732. https://doi.org/https://doi.org/10.1016/j.soildyn.2021.106732.

[10] Y.T. Guo, D. V Bompa, A.Y. Elghazouli, Nonlinear numerical assessments for the in-plane response of historic masonry walls, Eng. Struct. 268 (2022) 114734. https://doi.org/https://doi.org/10.1016/j.engstruct.2022.114734.

[11] M.F. Funari, A. Mehrotra, P.B. Lourenço, A Tool for the Rapid Seismic Assessment of Historic Masonry Structures Based on Limit Analysis Optimisation and Rocking Dynamics, Appl. Sci. 11 (2021) 942. https://doi.org/10.3390/app11030942.

[12] A. Mehrotra, M.J. DeJong, A CAD-interfaced dynamics-based tool for analysis of masonry collapse mechanisms, Eng. Struct. 172 (2018) 833–849. https://doi.org/10.1016/j.engstruct.2018.06.053.

[13] M.F. Funari, L.C. Silva, N. Savalle, P.B. Lourenço, A concurrent micro/macro FE-model optimized with a limit analysis tool for the assessment of dry-joint masonry structures, Int. J. Multiscale Comput. Eng. In Press (2022). https://doi.org/10.1615/IntJMultCompEng.2021040212.

[14] A. Giuffrè, Letture sulla meccanica delle murature storiche, Kappa, 1991.

[15] C. Casapulla, L.U. Argiento, A. Maione, E. Speranza, Upgraded formulations for the onset of local mechanisms in multi-storey masonry buildings using limit analysis, in: Structures, Elsevier, 2021: pp. 380–394.

[16] M.F. Funari, B. Pulatsu, S. Szabó, P.B. Lourenço, A Solution for the Frictional Resistance in Macro-Block Limit Analysis of Non-periodic Masonry, Structures. (2022).

[17] E. Mele, A. De Luca, A. Giordano, Modelling and analysis of a basilica under earthquake loading, J. Cult. Herit. 4 (2003) 355–367. https://doi.org/10.1016/j.culher.2003.03.002.

[18] M. Betti, L. Galano, Seismic analysis of historic masonry buildings: The Vicarious Palace in Pescia (Italy), Buildings. 2 (2012) 63–82. https://doi.org/10.3390/buildings2020063.

[19] A.M. D'Altri, N. Lo Presti, N. Grillanda, G. Castellazzi, S. de Miranda, G. Milani, A two-step automated procedure based on adaptive limit and pushover analyses for the seismic assessment of masonry structures, Comput. Struct. 252 (2021) 106561. https://doi.org/10.1016/j.compstruc.2021.106561.

[20] S. Szabó, M.F. Funari, P.B. Lourenço, Masonry patterns' influence on the damage assessment of URM walls: Current and future trends, Dev. Built Environ. 13 (2023) 100119. https://doi.org/https://doi.org/10.1016/j.dibe.2023.100119.

[21] M. Gilbert, C. Casapulla, H.M. Ahmed, Limit analysis of masonry block structures with non-associative frictional joints using linear programming, Comput. Struct. 84 (2006) 873–887.

[22] M.C. Ferris, F. Tin-Loi, Limit analysis of frictional block assemblies as a mathematical program with complementarity constraints, Int. J. Mech. Sci. 43 (2001) 209–224.

[23] N.A. Nodargi, C. Intrigila, P. Bisegna, A variational-based fixed-point algorithm for the limit analysis of dry-masonry block structures with non-associative Coulomb friction, Int. J. Mech. Sci. 161–162 (2019). https://doi.org/10.1016/j.ijmecsci.2019.105078.